

**Boronization Study for Application to Large
Helical Device**

**N. Noda, A. Sagara, H. Yamada, Y. Kubota,
N. Inoue, K. Akaishi, O. Motojima, K. Iwamoto,
M. Hashiba, I. Fujita, T. Hino, T. Yamashina,
K. Okazaki, J. Rice, M. Yamage, H. Toyoda
and H. Sugai**

(Received - July 8, 1994)

NIFS-292

July 1994

This report was prepared as a preprint of work performed as a collaboration research of the National Institute for Fusion Science (NIFS) of Japan. This document is intended for information only and for future publication in a journal after some rearrangements of its contents.

Inquiries about copyright and reproduction should be addressed to the Research Information Center, National Institute for Fusion Science, Nagoya 464-01, Japan.

Boronization Study for Application to Large Helical Device

N. Noda, A. Sagara, H. Yamada, Y. Kubota, N. Inoue, K. Akaishi,
O. Motojima,

K. Iwamoto¹, M. Hashiba¹, I. Fujita¹, T. Hino¹, T. Yamashina¹,
K. Okazaki², J. Rice³, M. Yamage⁴, H. Toyoda⁴, H. Sugai⁴

National Institute for Fusion Science, Nagoya 464-01, Japan

¹ *Faculty of Engineering, Hokkaido University, Sapporo 060, Japan*

² *The Institute of Physical and Chemical Research, Wako-shi,
350-01, Japan*

³ *Plasma Fusion Center, MIT, Cambridge, MA 02139, USA*

⁴ *Faculty of Engineering, Nagoya University, Nagoya 464-01, Japan*

Abstract

An experimental device named SUT (Surface modification Teststand) was constructed for a boronization study. An ultra high vacuum (UHV) condition, a changeable high temperature liner and *in-situ* AES are three distinctive feature of the SUT device.

Saturation density of oxygen atoms was as large as 1.2×10^{17} /cm² on a boronized surface, whereas 1.5×10^{16} /cm² on a bare stainless steel surface. It is found by AES analysis that the oxygen-contained layer was as thick as 50 nm from the top surface of the boron film. From such a large oxygen-saturation density, we expect that the oxygen-gettering ability of the boronized surface is likely to be maintained during one-day experiment of LHD.

The oxygen-saturation behavior was quite similar between the boronized surfaces obtained with decaborane and diborane, which indicates that, as a working gas of the boronization, the decaborane works well compared with diborane, as far as oxygen gettering is concerned.

Key Words : boronization, wall conditioning, decaborane,
in-situ AES, LHD, oxygen capacity, oxygen gettering

1. Introduction

It has been demonstrated that boronization is effective to reduce oxygen contamination to tokamak and helical plasmas [1, 2]. Reduction of oxygen results in wider operational range of Ohmically heated plasmas in tokamaks, and of ECH plasmas in helical devices [1, 3]. For instance, oxygen concentration is reduced to less than 1 % in TEXTOR after boronization, and the density limit rose up to $6 \times 10^{19} /\text{m}^3$ for OH discharges [4].

There are several problems with the boronization, such as hydrogen recycling control, life time of boron films, safety handling of diborane gas *etc.* from a practical point of view. Several questions are also risen for mechanism of the coating process, oxygen and hydrogen behavior with the boron coated layer, *etc.*

On the other hand, oxygen reduction is an important issue in Large Helical Device (LHD) [5], because the baking temperature is limited to 100°C [6]. Moreover, LHD will be operated with super-conducting magnetic coils, which means that a magnetic field as high as 3T is maintained between main discharges all the day. Then glow-discharge conditioning will not be available between high power shots, which has been routinely applied in DIII-D [7]. Thus a special effort is required to optimize the boronization technique in order to meet demands of the LHD operation.

Titanium flash is found to be one of effective procedures to reduce oxygen contamination in helical devices, such as CHS [3] and ATF [8]. One of the problems of the titanium gettering technique is that oxygen gettering ability is changing shot by shot after fresh titanium flash. Oxygen behavior with a boronized wall has been compared that with a titanium flashed wall, and it was found that the boronized wall is more promising than the titanium flashed wall [9].

In order to obtain a database necessary for the LHD boronization, we have started a series of experiments on boronization process and on behavior of hydrogen isotopes and oxygen impurity with boronized walls. Experimental results and preliminary discussions are given in this paper.

2. Apparatus

An experimental device named SUT (Surface modification Teststand, see Fig.1) has been constructed for this series of experiment. The main reaction chamber (MRC) is made of stainless steel. Inside MRC, a liner, which can be heated up to 600 °C, is installed. This liner can be easily replaced by another one after a series of experiments, and a new experiment can be started with a fresh liner with a clean surfacc.

An Auger Electron Spectroscopy (AES) system is set inside an analyzing chamber (ANC) attached to MRC. Samples exposed to a reacting plasma can be easily transferred between MRC and ANC by a swing-linear manipulator. By this system, depth profile of surface composition can be obtained without exposing samples to the air immediately after surface treatments in MRC.

The main chamber MRC is pumped with two turbo-molecular pumps (TMP) with a tandem arrangement. The chamber ANC is pumped by an ion pump. Base pressure in MRC and ANC is as low as $1 - 2 \times 10^{-7}$ Pa, which enables us to do precise analyses of oxygen behavior on surfaces.

Thus an ultra high vacuum (UHV) condition, a changeable high temperature liner and the *in-situ* AES are three distinctive feature of the SUT device.

Reacting gases are supplied through mass-flow controllers. A glow discharge in diborane or decaborane gas is used for boronization. Oxygen glow discharge is also applied to investigate its absorption by the liner surfaces. These reacting gases are usually supplied mixed with helium gas. A quartz oscillator is used to monitor the thickness of coating layers during and after boronization. A differentially pumped quadrupole residual gas analyzer (RGA) is installed for mass balance analyses of gaseous components inside the liner. An optical spectrometer of visible range is also used to investigate discharge processes.

3. Experimental results

One of the advantages of a boronized wall is that its surface works as an oxygen-getter and prevents oxygen atoms to recycle back into

plasmas. This effect reduces oxygen contamination in core plasmas similar to a titanium flashed wall in tokamaks and helical devices. A question is its lifetime as an oxygen-gettering surface. The lifetime of the boron film itself is expected to be considerably long for plasma-facing surfaces other than divertor stripes or limiters. However, the oxygen-gettering effect is presumed to disappear after the top surface of the boron film is saturated by oxygen atoms. In LHD, fresh boronization with a glow discharge is hardly applied in an interval of a series of one-day experiment because all the coils are superconducting magnet, and a magnetic field as strong as 3T is continuously applied all the day. Then less frequent boronization is desirable in LHD compared to the present devices. In order to estimate the lifetime of oxygen gettering ability, oxygen saturation of boronized surface has been investigated.

A glow discharge in a gas mixture of 10 % O₂ and 90% He was continued for around 1 hour with and without boronized surface. The liner was made of stainless steel (SUS304). The boronization was carried out by a glow discharge in a gas mixture of 10% B₂H₆ (diborane) and 90% He. The average thickness of the boron-coated layer was around 200 nm. The liner was kept at room temperature in the course of these processes, which corresponds to the operational condition expected to the LHD first wall. The partial pressure P_{32} of oxygen went down just after ignition of the glow discharge in O₂ + He. It recovered gradually with time and came back to the original level later. The partial pressure P_{28} , mainly contributed by CO, occasionally increased at the initial phase of the discharge. Net oxygen P_{OX} absorbed to the surface was obtained from the sum of $(P_{32} + 0.5P_{28})$ plotted in Fig. 2 as a function of time. It is clearly seen that the recovery of P_{OX} is quicker without boronization (*ig.* bare stainless steel wall) than with boronization. The RGA was calibrated to obtain the absolute partial pressures of O₂ and CO gases by comparing its signal level to that of a diaphragm gauge. Using these absolute pressure, the total number of the absorbed oxygen atoms can be calculated by integrating time behavior of P_{OX} . This was 1.5×10^{16} /cm² for a bare stainless steel surface, and 1.2×10^{17} /cm² for a boronized surface,

respectively. The similar concentration on a boronized surface has been observed already in the previous experiment in Nagoya University [10]. The direct comparison of the saturation density between a boronized and an un-boronized surface has been given for the first time in the present experiment. There is no doubt that a boronized surface absorbs an order of magnitude larger amount of oxygen atoms than the stainless steel surface. This number density was extremely large, which could be hardly understood as oxygen atoms existing within a few monolayer from the top surface of a boron film, which is expected from an implanted range with impact energy of oxygen ions from a glow discharge plasma.

In order to get the depth profile of the oxygen concentration, an *in-situ* AES analysis was performed for a oxygen-saturated boronized surface after one hour exposure to O₂/He discharge. The result is shown in Fig. 3. In the most part of the boron film, oxygen and carbon concentration was less than 2-3 at. %. Oxygen concentration was around 40% at the top surface, reduces as a function of the distance from the top surface. It can be seen that oxygen is penetrating up to 50 nm in depth. By integrating this depth profile, surface concentration of oxygen close to $1 \times 10^{17} / \text{cm}^2$ is obtained based on this result. This value of the surface concentration agreed with the one obtained by the RGA analysis within a factor of 2.

Thus both of the RGA and AES results support that, in contrast to a stainless steel surface, in which the saturated surface oxygen concentration is around $1 \times 10^{16} / \text{cm}^2$, oxygen atoms as much as $1 \times 10^{17} / \text{cm}^2$ can be absorbed in a boron-coated surface.

From the above result, we can expect that a boron-coated layer of 100 nm in thickness is sufficient as an oxygen-gettering surface. Oxygen capacity was measured as a function of the boron-film thickness and the result is shown in Fig. 4. The capacity is really saturated above 100 nm in thickness. In actual plasma experimental devices, non-uniformity in thickness is expected due to an arrangement of its boronization system. The minimum thickness should be ≈ 100 nm in those cases.

We are also interested in boronization with decaborane gas, which can be more safely handled than diborane [9]. We have compared the coating speed between these two schemes. It is about 5 times quicker

with decaborane gas than with diborane gas for the same gas-flow rate. This can be simply understood that a decaborane molecule contains 10 boron atoms whereas diborane does 2. The oxygen absorption capacity was compared between boronized films coated by glow discharges using these two gases. The thickness of the boron-coated layer was 210 nm with diborane and 135 nm with decaborane, both of which it exceeds 100 nm. The result is shown in Fig. 5. Time behaviors and absolute values of P_{OX} agreed each other quite well, which indicates that the decaborane works well compared with diborane as the working gas of the boronization, as far as oxygen gettering is concerned.

4. Discussion

Oxygen absorption capacity of boronized surface is considerably large. This is rather good from a practical view point, that is, the life time of the oxygen gettering ability is expected to be long. We have tried a rough estimation of the lifetime for an LHD case.

Firstly, we assume the severest case, in which all oxygen atoms are concentrated to the divertor-striking stripes. The LHD configuration has four divertor legs [11], and its total area A_{LHD} is around $1.0 \times 10^5 \text{ cm}^2$. Next, we assume the maximum surface density, namely the saturation density, of oxygen atoms C_{smax} as $1.2 \times 10^{17} \text{ cm}^2$, which is given from the results in Fig. 2. Thus the limiting oxygen number Q_{limit} is estimated to be

$$Q_{limit} \sim A_{LHD} C_{smax} = 1.0 \times 10^{22} \text{ cm}^2 .$$

The total number N_{Ox} of oxygen atoms which come out for a unit time to the divertor legs is given as

$$N_{Ox} / \tau_p = 0.005 n_e V_{LHD} / \tau_p = 1.0 \times 10^{19} \text{ cm}^2/\text{s} ,$$

where $V_{LHD} = 2.0 \times 10^7 \text{ cm}^3$ is the LHD plasma volume, τ_p the particle confinement time assumed to be 0.1 s , $n_e = 5.0 \times 10^{13} \text{ cm}^2/\text{s}$ a

plasma density given here. Average oxygen concentration inside the core plasma is assumed to be 0.5 %. The total number of oxygen atoms for 1 shot $Q_{[1shot]}$ is obtained as $Q_{[1shot]} = 5.0 \times 10^{20}$ for a 10 second discharge. The life time of the oxygen-gettering ability is estimated through dividing Q_{limit} by $[1shot]$, namely $1.2 \times 10^{22} / 5.0 \times 10^{20} \sim 24$ shots.

In the above estimation, it is assumed that all oxygen atoms are concentrated to the divertor-striking stripes. In real plasma devices, oxygen outflux is distributed to a wider area of its first wall. Although more precise data of τ_p are necessary for getting the lifetime, we can conclude based on the large capacity of oxygen on the boronized surface obtained in this experiment that the oxygen-gettering ability of the boronized surface is likely to be maintained during one-day experiment of LHD.

Another question is why the oxygen-absorption layer is so thick as 50 nm. From the impact energy of oxygen ions, presumed to be less than 400 V from the cathode sheath of glow-discharge, the range of the ions could be a few nm. In Fig. 2, gradual decrease can be seen in the oxygen concentration as a function of the distance from the top surface. These two facts suggest some "diffusion" or "erosion/deposition" process of oxygen after once implanted to the surface. The mechanism is not clear at present.

5. Summary

An experimental device named SUT (SURface modification Teststand) was constructed for a basic investigation of boronization process and boronized surfaces, aiming to optimize the boronization technique for the superconducting device of LHD. An ultra high vacuum (UHV) condition, a changeable high temperature liner and an *in-situ* AES are three distinctive feature of the SUT device.

Saturation density of oxygen atoms was measured for boronized surface. It was around $1.2 \times 10^{17} / \text{cm}^2$, which is much larger than the measured surface density on a bare stainless steel surface without boronization. This was confirmed by AES analysis, where it is found that

the oxygen-contained layer was as thick as 50 nm. The reason is not clear why oxygen is absorbed beyond the range of implantation depth with a glow discharge. Based on such large number of oxygen-saturation density, we can conclude that the oxygen-gettering ability of the boronized surface is likely to be maintained over one-day experiment of LHD.

Oxygen concentration was 40 % at the top surface of an oxygen-gettered surface for a boron layer after saturation by an O₂ + He glow discharge.

Decaborane and diborane boronization were compared in a similar condition. The oxygen-saturation behavior is quite similar between the boronized surfaces obtained with these two working gases. The coating speed is 5 times faster with decaborane than with diborane, which can be simply understood by taking into account the number ratio of oxygen atoms for both gases. This indicates that the decaborane works well compared with diborane as a working gas of the boronization, as far as oxygen gettering is concerned.

References

- [1] J. Winter, H.G. Esser et al., *J. Nucl. Mater.* **162-164** (1989) 713.
- [2] P. Grigull, R. Behrisch et al., *J. Nucl. Mater.* **196-198** (1992) 101.
- [3] N. Noda, S. Okamura et al., *J. Nucl. Mater.* **162-164** (1989) 640.
- [4] J. Winter, *J. Nucl. Mater.* **176&177** (1990) 14.
- [5] O. Motojima, K. Yamazaki et al., in *Plasma Physics and Controlled Fusion Research 1990*, Vol.3, IAEA, Vienne, 1991. P.513.
- [6] N. Noda and A. Iiyoshi, *Shinku* **36** (1993) 403 (in Japanese).
- [7] G. Jackson, J. Winter et al., *J. Nucl. Mater.* **196-198** (1992) 236.
- [8] R. C. Isler, G. L. Bell et al., *J. Nucl. Mater.* **176&177** (1990) 332.
- [9] H. Yamada et al., to be published in *Jpn. J. Appl. Phys.*
- [10] M. Yamage, T. Ejima, H. Toyoda and H. Sugai, *J. Nucl. Mater.* **196-198** (1992) 618.
- [11] N. Noda, Y. Kubota, A. Sagara et al., *Fusion Technology 1992* (ed. C. Ferro et al.), Elsevier, Amsterdam, p.325.

Figure Captions

- Fig. 1** Top view of the SUT device. A sample exposed to a reacting plasma can be transferred from the main chamber to analyzing chamber without exposing it to the air by a swing-linear manipulator.
- Fig. 2** Oxygen absorbed by a boronized (closed circles) and an unboronized wall (open circles) during an $O_2(10\%) + He(90\%)$ glow discharge. The absorbed amount is expressed by equivalent pressure with O_2 gas here.
- Fig. 3** Depth profile of the boronized surface after exposure to one hour discharge of oxidization (a glow discharge in an O_2/He mixture gas), obtained with the *in-situ* AES analysis.
- Fig. 4** Oxygen gettering capacity as a function of boron-film thickness.
- Fig. 5** Oxygen absorbed by a surface boronized a diborane glow discharge and by that with a decaborane discharge.

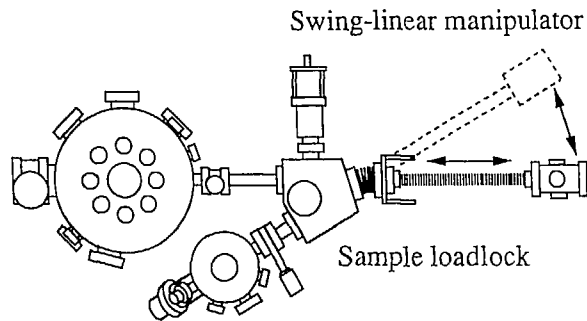


Fig. 1 Top view of the SUT device. A sample exposed to a reacting plasma can be transferred from the main chamber to analyzing chamber without exposing it to the air by a swing-linear manipulator.

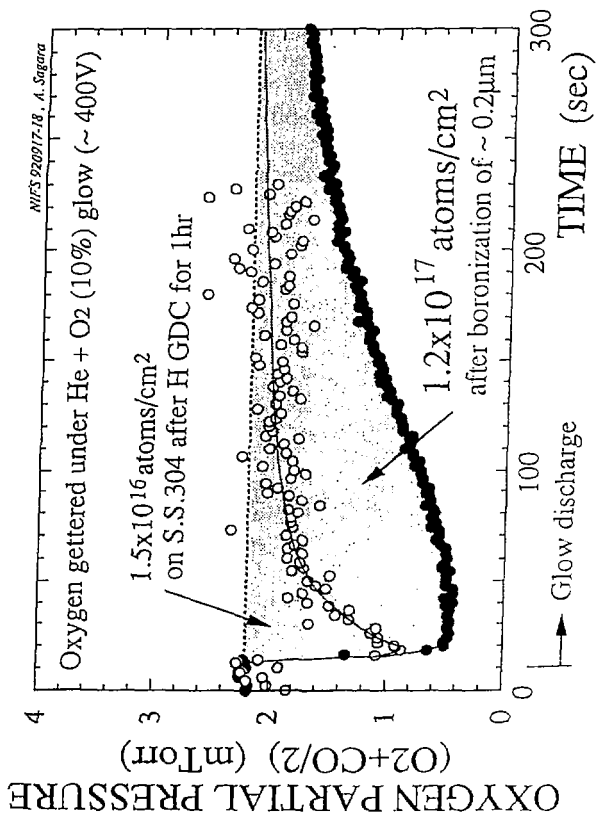


Fig. 2 Oxygen absorbed by a boronized (closed circles) and an unboronized wall (open circles) during an O₂(10%) + He(90%) glow discharge. The absorbed amount is expressed by equivalent pressure with O₂ gas here.

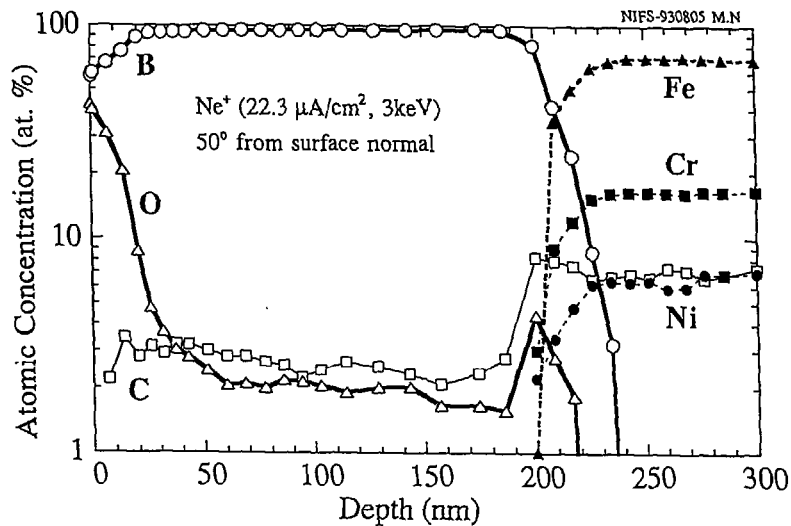


Fig. 3 Depth profile of the boronized surface after exposure to one hour discharge of oxidization (a glow discharge in an O₂/He mixture gas), obtained with the *in-situ* AES analysis.

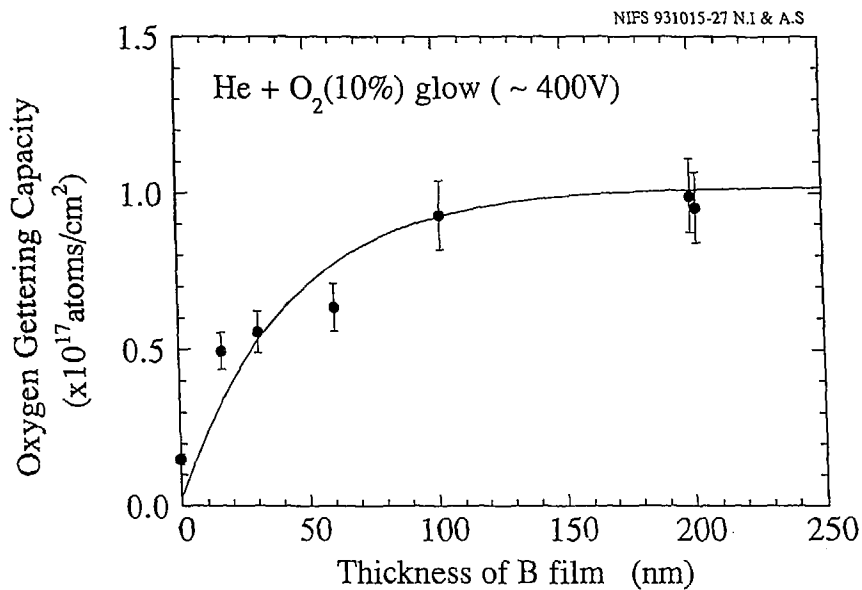


Fig. 4 Oxygen getting capacity as a function of boron-film thickness.

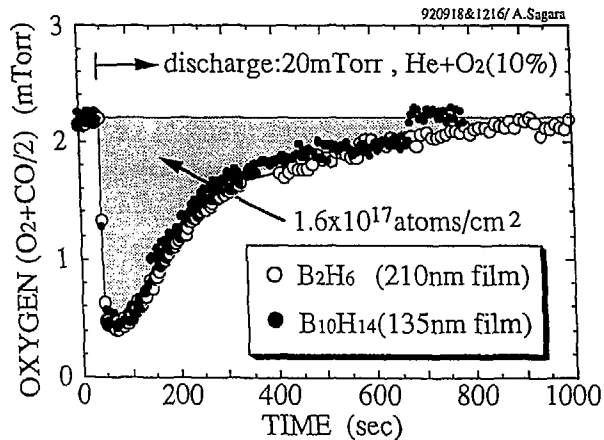


Fig. 5 Oxygen absorbed by a surface boronized diborane glow discharge and by that with a decaborane discharge.

Recent Issues of NIFS Series

- NIFS-248 Y. Kondoh,
Attractors of Dissipative Structure in Three Dissipative Fluids; Oct. 1993
- NIFS-249 S. Murakami, M. Okamoto, N. Nakajima, M. Ohnishi, H. Okada,
Monte Carlo Simulation Study of the ICRF Minority Heating in the Large Helical Device; Oct. 1993
- NIFS-250 A. Iiyoshi, H. Momota, O. Motojima, M. Okamoto, S. Sudo, Y. Tomita, S. Yamaguchi, M. Ohnishi, M. Onozuka, C. Uenosono,
Innovative Energy Production in Fusion Reactors; Oct. 1993
- NIFS-251 H. Momota, O. Motojima, M. Okamoto, S. Sudo, Y. Tomita, S. Yamaguchi, A. Iiyoshi, M. Onozuka, M. Ohnishi, C. Uenosono,
Characteristics of D-³He Fueled FRC Reactor: ARTEMIS-L, Nov. 1993
- NIFS-252 Y. Tomita, L.Y. Shu, H. Momota,
Direct Energy Conversion System for D-³He Fusion, Nov. 1993
- NIFS-253 S. Sudo, Y. Tomita, S. Yamaguchi, A. Iiyoshi, H. Momota, O. Motojima, M. Okamoto, M. Ohnishi, M. Onozuka, C. Uenosono,
Hydrogen Production in Fusion Reactors, Nov. 1993
- NIFS-254 S. Yamaguchi, A. Iiyoshi, O. Motojima, M. Okamoto, S. Sudo, M. Ohnishi, M. Onozuka, C. Uenosono,
Direct Energy Conversion of Radiation Energy in Fusion Reactor, Nov. 1993
- NIFS-255 S. Sudo, M. Kanno, H. Kaneko, S. Saka, T. Shirai, T. Baba,
Proposed High Speed Pellet Injection System "HIPEL" for Large Helical Device
Nov. 1993
- NIFS-256 S. Yamada, H. Chikaraishi, S. Tanahashi, T. Mito, K. Takahata, N. Yanagi, M. Sakamoto, A. Nishimura, O. Motojima, J. Yamamoto, Y. Yonenaga, R. Watanabe,
Improvement of a High Current DC Power Supply System for Testing the Large Scaled Superconducting Cables and Magnets; Nov. 1993
- NIFS-257 S. Sasaki, Y. Uesugi, S. Takamura, H. Sanuki, K. Kadota,
Temporal Behavior of the Electron Density Profile During Limiter Biasing in the HYBTOK-II Tokamak; Nov. 1993
- NIFS-258 K. Yamazaki, H. Kaneko, S. Yamaguchi, K.Y. Watanabe, Y. Taniguchi, O. Motojima, LHD Group,
Design of Central Control System for Large Helical Device (LHD);

Nov. 1993

- NIFS-259 S. Yamada, T. Mito, A. Nishimura, K. Takahata, S. Satoh, J. Yamamoto, H. Yamamura, K. Masuda, S. Kashihara, K. Fukusada, E. Tada, *Reduction of Hydrocarbon Impurities in 200L/H Helium Liquefier-Refrigerator System*; Nov. 1993
- NIFS-260 B.V.Kuteev, *Pellet Ablation in Large Helical Device*; Nov. 1993
- NIFS-261 K. Yamazaki, *Proposal of "MODULAR HELIOTRON": Advanced Modular Helical System Compatible with Closed Helical Divertor*; Nov. 1993
- NIFS-262 V.D.Pustovitov, *Some Theoretical Problems of Magnetic Diagnostics in Tokamaks and Stellarators*; Dec. 1993
- NIFS-263 A. Fujisawa, H. Iguchi, Y. Hamada *A Study of Non-Ideal Focus Properties of 30° Parallel Plate Energy Analyzers*; Dec. 1993
- NIFS-264 K. Masai, *Nonequilibrium in Thermal Emission from Supernova Remnants*; Dec. 1993
- NIFS-265 K. Masai, K. Nomoto, *X-Ray Enhancement of SN 1987A Due to Interaction with its Ring-like Nebula*; Dec. 1993
- NIFS-266 J. Uramoto *A Research of Possibility for Negative Muon Production by a Low Energy Electron Beam Accompanying Ion Beam*; Dec. 1993
- NIFS-267 H. Iguchi, K. Ida, H. Yamada, K. Itoh, S.-I. Itoh, K. Matsuoka, S. Okamura, H. Sanuki, I. Yamada, H. Takenaga, K. Uchino, K. Muraoka, *The Effect of Magnetic Field Configuration on Particle Pinch Velocity in Compact Helical System (CHS)*; Jan. 1994
- NIFS-268 T. Shikama, C. Namba, M. Kosuda, Y. Maeda, *Development of High Time-Resolution Laser Flash Equipment for Thermal Diffusivity Measurements Using Miniature-Size Specimens*; Jan. 1994
- NIFS-269 T. Hayashi, T. Sato, P. Merkel, J. Nührenberg, U. Schwenn, *Formation and 'Self-Healing' of Magnetic Islands in Finite- β Helias Equilibria*; Jan. 1994

- NIFS-270 S. Murakami, M. Okamoto, N. Nakajima, T. Mutoh,
Efficiencies of the ICRF Minority Heating in the CHS and LHD Plasmas; Jan. 1994
- NIFS-271 Y. Nejob, H. Sanuki,
Large Amplitude Langmuir and Ion-Acoustic Waves in a Relativistic Two-Fluid Plasma; Feb. 1994
- NIFS-272 A. Fujisawa, H. Iguchi, A. Taniike, M. Sasao, Y. Hamada,
A 6MeV Heavy Ion Beam Probe for the Large Helical Device;
Feb. 1994
- NIFS-273 Y. Hamada, A. Nishizawa, Y. Kawasumi, K. Narihara, K. Sato, T. Seki,
K. Toi, H. Iguchi, A. Fujisawa, K. Adachi, A. Ejiri, S. Hidekuma,
S. Hirokura, K. Ida, J. Koong, K. Kawahata, M. Kojima, R. Kumazawa,
H. Kuramoto, R. Liang, H. Sakakita, M. Sasao, K. N. Sato, T. Tsuzuki,
J. Xu, I. Yamada, T. Watari, I. Negi,
Measurement of Profiles of the Space Potential in JIPP T-IIU Tokamak Plasmas by Slow Poloidal and Fast Toroidal Sweeps of a Heavy Ion Beam; Feb. 1994
- NIFS-274 M. Tanaka,
A Mechanism of Collisionless Magnetic Reconnection; Mar. 1994
- NIFS-275 A. Fukuyama, K. Itoh, S.-I. Itoh, M. Yagi and M. Azumi,
Isotope Effect on Confinement in DT Plasmas; Mar. 1994
- NIFS-276 R.V. Reddy, K. Watanabe, T. Sato and T.H. Watanabe,
Impulsive Alfvén Coupling between the Magnetosphere and Ionosphere; Apr. 1994
- NIFS-277 J. Uramoto,
A Possibility of π^- Meson Production by a Low Energy Electron Bunch and Positive Ion Bunch; Apr. 1994
- NIFS-278 K. Itoh, S.-I. Itoh, A. Fukuyama, M. Yagi and M. Azumi,
Self-sustained Turbulence and L-mode Confinement in Toroidal Plasmas II; Apr. 1994
- NIFS-279 K. Yamazaki and K.Y. Watanabe,
New Modular Heliotron System Compatible with Closed Helical Divertor and Good Plasma Confinement; Apr. 1994
- NIFS-280 S. Okamura, K. Matsuoka, K. Nishimura, K. Tsumori, R. Akiyama,
S. Sakakibara, H. Yamada, S. Morita, T. Morisaki, N. Nakajima,
K. Tanaka, J. Xu, K. Ida, H. Iguchi, A. Lazaros, T. Ozaki, H. Arimoto,
A. Ejiri, M. Fujiwara, H. Idei, O. Kaneko, K. Kawahata, T. Kawamoto,
A. Komori, S. Kubo, O. Motojima, V.D. Pustovitov, C. Takahashi, K. Toi
and I. Yamada,

High-Beta Discharges with Neutral Beam Injection in CHS,
Apr; 1994

- NIFS-281 K. Kamada, H. Kinoshita and H. Takahashi,
Anomalous Heat Evolution of Deuteron Implanted Al on Electron Bombardment ; May 1994
- NIFS-282 H. Takamaru, T. Sato, K. Watanabe and R. Horiuchi,
Super Ion Acoustic Double Layer; May 1994
- NIFS-283 O.Mitarai and S. Sudo
Ignition Characteristics in D-T Helical Reactors; June 1994
- NIFS-284 R. Horiuchi and T. Sato,
Particle Simulation Study of Driven Magnetic Reconnection in a Collisionless Plasma; June 1994
- NIFS-285 K.Y. Watanabe, N. Nakajima, M. Okamoto, K. Yamazaki, Y. Nakamura, M. Wakatani,
Effect of Collisionality and Radial Electric Field on Bootstrap Current in LHD (Large Helical Device); June 1994
- NIFS-286 H. Sanuki, K. Itoh, J. Todoroki, K. Ida, H. Idei, H. Iguchi and H. Yamada,
Theoretical and Experimental Studies on Electric Field and Confinement in Helical Systems; June 1994
- NIFS-287 K. Itoh and S.-I. Itoh,
Influence of the Wall Material on the H-mode Performance;
June 1994
- NIFS-288 K. Itoh, A. Fukuyama, S.-I. Itoh, M. Yagi and M. Azumi
Self-Sustained Magnetic Braiding in Toroidal Plasmas
July 1994
- NIFS-289 Y. Nejoh,
Relativistic Effects on Large Amplitude Nonlinear Langmuir Waves in a Two-Fluid Plasma; July 1994
- NIFS-290 N. Ohyaibu, A. Komori, K. Akaishi, N. Inoue, Y. Kubota, A.I. Livshit, N. Noda, A. Sagara, H. Suzuki, T. Watanabe, O. Motojima, M. Fujiwara, A. Iiyoshi,
Innovative Divertor Concepts for LHD; July 1994
- NIFS-291 H. Idei, K. Ida, H. Sanuki, S. Kubo, H. Yamada, H. Iguchi, S. Morita, S. Okamura, R. Akiyama, H. Arimoto, K. Matsuoka, K. Nishimura, K. Ohkubo, C. Takahashi, Y. Takita, K. Toi, K. Tsumori and I. Yamada,
Formation of Positive Radial Electric Field by Electron Cyclotron Heating in Compact Helical System; July 1994